Research Article | Vol. 9, No. 12 | 1 Dec 2018 | BIOMEDICAL OPTICS EXPRESS 5939
Biomedical Optics EXPRESS

Live-cell imaging of human spermatozoa using structured illumination microscopy

IDA S. OPSTAD,[1,5] DARIA A. POPOVA,[2,5] GANESH ACHARYA,[2,3] PURUSOTAM BASNET,[2,4] AND BALPREET S. AHLUWALIA[1,*]

[1]*Department of Physics and Technology, UiT The Arctic University of Norway, 9037 Tromsø, Norway*
[2]*Women's Health and Perinatology Research Group, Department of Clinical Medicine, UiT The Arctic University of Norway, Tromsø, Norway*
[3]*Department of Clinical Science, Intervention & Tech. Karolinska Institutet, Stockholm, Sweden*
[4]*IVF Unit, Department of Obstetrics & Gynecology, University Hospital North Norway, Tromsø, Norway*
[5]*Both authors contributed equally to this work*
[*]*balpreet.singh.ahluwalia@uit.no*

Abstract: Structural details of spermatozoa are interesting from the perspectives of fundamental biology and growing reproductive health problems. Studies of nanostructural details of these extremely motile cells have been limited to fixed cells, largely using electron microscopy. Here we provide the protocols for and demonstrate live-cell multi-color super-resolution imaging of human spermatozoa using structured illumination microscopy (SIM). By using patches of agarose for immobilization, we achieved four-channel 3D SIM imaging of the plasma membrane, nucleus, mitochondria and microtubulin in the same living sperm cells. We expect that high-resolution imaging of living spermatozoa will be implemented for research on fundamental cellular mechanisms together with morphological aberrations involved in male infertility for a future improved cell selection process in in vitro fertilization treatments.

1. Introduction

Research on subcellular organization of human reproductive cells and preimplantation embryos is becoming increasing popular as it is considered to be important to tackle growing reproductive health problems. Along with female infertility, male factor infertility is a significant issue which may result from different causes, such as anatomical anomalies, hormonal imbalances, infections or genetic abnormalities. However, the etiology of male infertility remains undiagnosed in about one third of the cases [1,2]. Nowadays, male reproductive health assessment is primarily based on sperm quality, and morphology is one of the main characteristics evaluated in clinical practice. Changes in the ultrastructure and general morphology of sperm cells serves as an indicator of the influence of different physical (e.g. freezing in reproductive technologies) [3,4], chemical (occupational exposure to toxic substances) or environmental factors on semen reflecting male reproductive health during life [5,6].

Until recently, numerous studies have been performed to study the ultrastructure of sperm cells using transmission electron microscopy (TEM) to obtain high resolution images [3,7–9]. Compared to TEM, optical microscopy often enables the analysis of living cells, resulting in the elimination of artifacts specific to cell fixation, such as changed protein conformation with associated loss of staining specificity [10,11]. Though a valuable tool, the diffraction limit renders conventional light microscopy unable to resolve details finer than about 250 nm laterally and 500 nm axially using a high-end microscope. Optical nanoscopy (or super-resolution optical microscopy) encompass an array of techniques for overcoming the resolution limit of conventional microscopy, opening avenues for studying biological samples

#335318 https://doi.org/10.1364/BOE.9.005939
Journal © 2018 Received 15 Jun 2018; revised 14 Sep 2018; accepted 2 Oct 2018; published 5 Nov 2018

Biomedical Optics EXPRESS

in much greater detail than previously possible without the extensive sample preparation required for electron microscopy [12].

Structured illumination microscopy (SIM) is a live-cell compatible super-resolution technique that achieves greatly enhanced contrast along with a factor of two resolution enhancement in all three spatial dimensions as compared to the diffraction limit [13]. For biological structures just below the conventional resolution limit, SIM can thus be applied as a tool for valuable additional structural information in living cells. In the case of sperm cells, structural analysis using multi-color SIM offers opportunities for a more precise description of disease specific defects responsible for infertility, like morphological aberrations associated with teratozoospermia [14] or asthenozoospermia [15,16]. In addition to a better description of morphology, we expect that live-cell studies of sperm cells at super-resolution and enhanced contrast will contribute to a gain in knowledge about fundamental cellular mechanisms that might be implemented for an improved reproductive cell selection process in future in vitro fertilization (IVF) treatments.

The biggest hurdle for live-cell high-resolution imaging of sperm cells has been the extreme motility associated with their progressive swimming (~66 µm/s [17]), in addition to their free-floating nature as suspension cells. Until now, to the best of our knowledge, all super-resolution imaging of human spermatozoa has been limited to fixed cells. Other challenges associated with multi-color super-resolution microscopy of any cell type are labeling, label induced toxicity and phototoxicity. Here we provide a methodology for overcoming above-mentioned hurdles and demonstrate up to four-channel 3D SIM imaging of different sub-cellular structures in living human spermatozoa. We also provide labeling protocols and discuss associated challenges and opportunities.

2. Materials and methods

2.1 Sample preparation

Semen preparation

The Regional Committee for Medical and Health Research Ethics of Norway (REK-Nord) approved the project. Experiments were performed using semen of donors from the IVF clinic of the University Hospital of North Norway, Tromsø, Norway. All participants signed a written informed consent. Semen samples were collected according to the guidelines of the World Health Organization (WHO) with an abstinence period of 3–5 days.

After liquefaction, semen samples were examined using light microscopy and Neubauer-improved counting chambers. In the experiments, all samples contained no less than 60 million cells per milliliter and had progressive motility >50%. The swim up method was used to wash the samples. The semen samples were diluted with 5 mL of sperm washing medium (Sage) and centrifuged for 10 min at 700 x g. Supernatant was removed and the pellet was washed again. After removing the supernatant, 0.5 mL of swim up medium was layered and the tube was put into an incubator (5.0% CO_2, 37°C). During 60 min of incubation, highly motile spermatozoa migrated to the above layered medium. After incubation, the supernatant was aspirated with pipette, centrifuged and the sediment was used for the following procedures.

Labeling, immobilization and imaging conditions

Labeling and imaging were done at room temperature (~23°C) in PBS or Live Cell Imaging Solution (Molecular Probes) as summarized in Table 1. For multi-color experiments, the label requiring the longest incubation time was added to the cells first, and then sequentially the rest of the probes, so that at the end of the incubation time, the cells had been subjected to approximately the concentrations and labeling times as listed in Table 1. After incubation with the labels, the samples were diluted in PBS (~1:15) and spun down using 800 x g for 10 min. The supernatant was removed and the samples resuspended in PBS to a concentration

Biomedical Optics EXPRESS

found suitable for the respective sample and experiment. Drops of about 8 µL were placed on coverslips (#1.5 washed in 100% ethanol and placed in sample holders for live-cell microscopy) and covered with refrigerated patches of ~2% agarose (High-resolution, Sigma-Aldrich) in PBS. When the cells after a couple of minutes had become fully immobilized, the samples were covered with a plastic lid to prevent further drying during imaging. SiR-tubulin was purchased from Spirochrome (Cytoskeleton kit), while all other probes were purchased from Thermo Fisher Scientific.

Table 1. Labeling conditions applied for SIM imaging

Label	Concentration	Incubation time
CellMask Orange	1:1000	10 min
MitoTracker Green	200 nM	20 min
Hoechst 34580	5 µg/mL	20 min
SiR-tubulin	1 µM	2 h

2.2 Microscope

Images were acquired using a DeltaVision OMX V4 Blaze imaging system (GE Healthcare) equipped with a 60X 1.42NA oil-immersion objective (Olympus), three sCMOS cameras, and 405, 488, 568, and 642 nm lasers for excitation. The vendor specified optical resolution of the system (3D SIM) is 110-160 nm laterally, and 340-380 nm axially, depending on color channel. To surpass the diffraction limit, this SIM set-up uses sinusoidal illumination patterns and acquires 120 images per 1 µm z-stack thickness (3 illumination angles times 5 phase shifts times 8 planes/µm thickness) per color channel. Super-resolution 3D images are then obtained via image processing using the reconstruction software described below.

2.3 Image processing

Deconvolution and 3D SIM image reconstruction were completed using the manufacturer-supplied SoftWoRx program (GE Healthcare). Image registration (color alignment) was also performed in SoftWoRx using experimentally-measured calibration values compensating for minor lateral and axial shifts, rotation, and magnification differences between cameras. Further image processing was done using Fiji/ImageJ [18]

3. Results and discussion

3.1 Single-color imaging and immobilization

Immobilization using patches of agarose made high-resolution imaging of living spermatozoa possible. Figure 1 shows fluorescence microscopy images of living spermatozoa acquired using deconvolution microscopy (upper panel) and SIM (lower panel) for various live-cell compatible probes (CellMask Orange, panels (a) and (e); MitoTracker Green, panels (b) and (f); Hoechst 34580, panels (c) and (g); SiR-tubulin, panels (d) and (h)). The contrast and resolution enhancement for SIM compared to conventional deconvolution microscopy is apparent for all structures, but most prominent for the mitochondria-containing mid-piece, panels (a), (b), (e) and (f), where structures around 100 nm length-scale are prominent. For the nucleus, only minor contrast enhancement is visible, while for microtubulin (panels (d) and (h)) the resolution doubling provided by SIM makes it evident that the centriole (indicated by arrows) is completely separated from the rest of the axoneme.

Imaging from below through the coverslip (and not through the agarose) resulted in images not significantly affected by the agarose with absorbed leftover dye. Imaging a few planes below the agarose enabled us to acquire high quality SIM images of *most of* the living sperm cells, although not for the uppermost part (0.2 - 0.3 µm) of the cells, which was stuck in the agarose. To illustrate, the sample plane in Fig. 2(a) is unusable because of the signal from the agarose (with absorbed leftover dye), while for the neighboring sample planes shown in Fig. 2(b) and 2(c), the agarose is now above and not in the image plane, enabling us

Biomedical Optics EXPRESS

to observe the cell at high resolution and contrast. In the particular cell depicted, an abnormally `puffed up' membrane morphology is revealed, clearly different from the tightly wrapped membrane in e.g. Fig. 1(e).

Though immobilization for live-cell microscopy using patches of agarose (often combined with cell growth medium) is widely applied in microbiology (e.g. discussed in [19]), this technique is not extensively used in the 'eukaryotic cell community'. We expect this immobilization technique applied here successfully for SIM of spermatozoa to be also directly applicable to other types of suspension cells that are challenging to image live otherwise. The addition of an agarose patch on top of the sample is suitable for imaging set-ups where both illumination and detection are conducted through the coverslip (and not through the agarose), as is often the case in fluorescence microscopy.

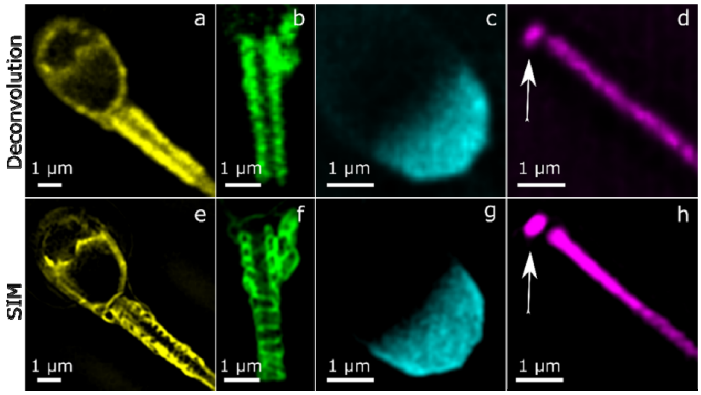

Fig. 1. Comparison of deconvolution microscopy (upper panels) and SIM (lower panels) images of living human spermatozoa for different probes. (a), (e) Plasma membrane labeled using CellMask Orange; (b), (f) Mitochondria labeled using MitoTracker Green; (c), (g) Nucleus labeled using Hoechst 34580; (d), (h) Microtubulin labeled using SiR-tubulin. The contrast and resolution enhancement are apparent for all probes, but most significant for the region containing mitochondria (panels (a), (b), (e) and (f)), but also for the centriole, indicated by arrows in panels (d) and (h). The images are single z-sections.

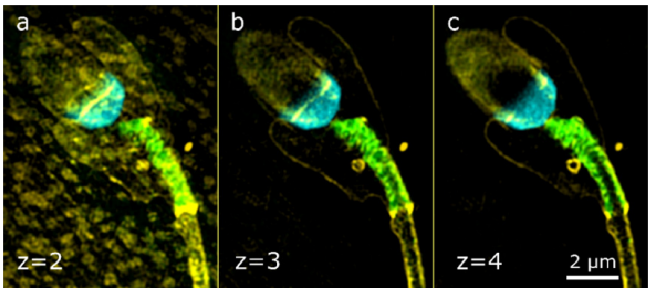

Fig. 2. Comparison of background signal in z-planes 2 (a), 3 (b) and 4 (c) counted from the agarose patch (top) used for immobilization. The distance between the z-slices is 125 nm. The agarose patch (with absorbed leftover dye) only causes significant background signal in the uppermost planes. The cells were labeled using CellMask Orange, MitoTracker Green and Hoechst 34580 and imaged live using SIM.

Biomedical Optics EXPRESS

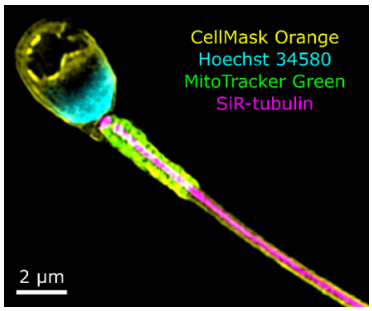

Fig. 3. Four-channel SIM image of living human spermatozoa labeled using CellMask Orange (yellow), MitoTracker Green (green), Hoechst 34580 (turquoise) and SiR-tubulin (magenta). The image is a 1 µm maximum intensity projected z-stack.

3.2 Multi-color SIM imaging

Figure 3 shows a four-channel SIM image of living human spermatozoa labeled using CellMask Orange, MitoTracker Green, Hoechst and SiR-tubulin. CellMask (yellow) labels the plasma membrane and outlines the entire cell, MitoTracker (green) labels mitochondria in the mid-piece clutching around the axoneme labeled using SiR-tubulin (magenta). Hoechst (cyan) labels DNA and is here visible only in the lower part of the head. For multi-color experiments, similar concentrations and labeling times were applicable as described for the single-probe experiments, though the labels were added sequentially to fit their individually optimized labeling time (with a single washing step in the end), resulting in slightly varying concentrations compared to the single-color experiments. Multi-color super-resolution imaging of living sperm cells unlocks exciting new possibilities regarding detailed analysis of subcellular structures for various cellular conditions, that can be employed to e.g. better understand diseases and the effect of different treatments in the field of reproductive medicine.

Four-channel SIM imaging of living cells is in general challenging for four reasons in particular: sample movement, photobleaching, phototoxicity, and depth-induced spherical aberrations. Sample movement was effectively eliminated using agarose patches. Photobleaching was countered using high labeling concentrations of bright photostable dyes with lowered illumination intensities and instead longer exposure times (20-30 ms) to ensure sufficient modulation contrast of the illumination pattern. Phototoxicity was not found problematic for these experiments as only single time-points were considered, although the four-channel imaging time for a 1.5 µm z-stack was around 20 s. Spherical aberrations were mitigated in these samples, through optimization of the immersion oil refractive index in use (1.516 was found appropriate for the four-channel imaging experiments), the tenuity of the samples (~0.5 – 3 µm thickness) and the sample placement directly on the coverslip. For thicker samples, spherical aberrations often cause SIM reconstruction artifacts, as the sample-induced aberrations can only be optimally corrected for one channel at a time.

4. Conclusions and summary

We provide a methodology for live-cell imaging of human spermatozoa using SIM, which is also applicable for a wide variety of other types of suspension cells and for imaging techniques where both illumination and detection are conducted through the coverslip. Labeling with fluorescent probes compatible with live-cell imaging, and subsequent immobilization using patches of agarose, enabled up to four-channel SIM imaging that revealed an unprecedented level of structural details of living sperm cells. This methodology shows great promise for shedding new light on sub-cellular structures and cellular mechanisms of the male reproductive cell in both healthy and diseased subjects, as live-cell imaging at super-resolution enables a much more precise description of e.g. morphological

Biomedical Optics EXPRESS

aberrations responsible for infertility. As compared to electron microscopy, the proposed methodology not only enables live-cell experiments, but also eliminates fixation steps and fixation related artefacts. This enables reduced sample preparation time and allows for multi-channel colocalization experiments by means of standard labeling protocols. In addition to a better description of morphology, we expect that live-cell studies of sperm cells at high resolution and contrast will contribute to an increased knowledge of fundamental cellular mechanisms that might be implemented for an improved reproductive cell selection process in IVF treatments in the future.

Funding

UiT, The Arctic Univeristy of Norway, Tematiske Satsinger program.

Acknowledgments

We would like to thank the men who provided semen samples and bioengineers: Ms. Sissle A. Hansen, Ms. Inger K. Olaussen and Ms. Sylvi Johansen at the IVF Clinic, University Hospital of North Norway, Tromsø for coordinating with the patients. The publication charges for this article have been funded by a grant from the publication fund of UiT The Arctic University of Norway.

Disclosures

The authors declare that there are no conflicts of interest related to this article.

References

1. G. Cavallini, "Male idiopathic oligoasthenoteratozoospermia," Asian J. Androl. **8**(2), 143–157 (2006).
2. N. Kumar and A. K. Singh, "Trends of male factor infertility, an important cause of infertility: A review of literature," J. Hum. Reprod. Sci. **8**(4), 191–196 (2015).
3. S. Ozkavukcu, E. Erdemli, A. Isik, D. Oztuna, and S. Karahuseyinoglu, "Effects of cryopreservation on sperm parameters and ultrastructural morphology of human spermatozoa," J. Assist. Reprod. Genet. **25**(8), 403–411 (2008).
4. C. Barthelemy, D. Royere, S. Hammahah, C. Lebos, M. J. Tharanne, and J. Lansac, "Ultrastructural changes in membranes and acrosome of human sperm during cryopreservation," Arch. Androl. **25**(1), 29–40 (1990).
5. N. Naha, R. B. Bhar, A. Mukherjee, and A. R. Chowdhury, "Structural alteration of spermatozoa in the persons employed in lead acid battery factory," Indian J. Physiol. Pharmacol. **49**(2), 153–162 (2005).
6. W. Asghar, H. Shafiee, V. Velasco, V. R. Sah, S. Guo, R. El Assal, F. Inci, A. Rajagopalan, M. Jahangir, R. M. Anchan, G. L. Mutter, M. Ozkan, C. S. Ozkan, and U. Demirci, "Toxicology Study of Single-walled Carbon Nanotubes and Reduced Graphene Oxide in Human Sperm," Sci. Rep. **6**(1), 30270 (2016).
7. D. Lacy, A. J. Pettitt, J. M. Pettitt, and B. S. Martin, "Application of scanning electron microscopy to semen analysis of the sub-fertile man utilising data obtained by transmission electron microscopy as an aid to interpretation," Micron (1969) **5**(2), 135–173 (1974).
8. B. Baccetti, S. Capitani, G. Collodel, G. Di Cairano, L. Gambera, E. Moretti, and P. Piomboni, "Genetic sperm defects and consanguinity," Hum. Reprod. **16**(7), 1365–1371 (2001).
9. E. H. Chemes and Y. V. Rawe, "Sperm pathology: a step beyond descriptive morphology. Origin, characterization and fertility potential of abnormal sperm phenotypes in infertile men," Hum. Reprod. Update **9**(5), 405–428 (2003).
10. A. J. Hobro and N. I. Smith, "An evaluation of fixation methods: Spatial and compositional cellular changes observed by Raman imaging," Vib. Spectrosc. **91**, 31–45 (2017).
11. J. Kiernan, *Formaldehyde, Formalin, Paraformaldehyde And Glutaraldehyde: What They Are And What They Do* (2000).
12. C. G. Galbraith and J. A. Galbraith, "Super-resolution microscopy at a glance," J. Cell Sci. **124**(10), 1607–1611 (2011).
13. R. Heintzmann and T. Huser, "Super-Resolution Structured Illumination Microscopy," Chem. Rev. **117**(23), 13890–13908 (2017).
14. E. Moretti, and G. Collodel, *Electron Microscopy in the Study of Human Sperm Pathologies* (2012).
15. V. Y. Rawe, G. D. Galaverna, A. A. Acosta, S. B. Olmedo, and H. E. Chemes, "Incidence of tail structure distortions associated with dysplasia of the fibrous sheath in human spermatozoa," Hum. Reprod. **16**(5), 879–886 (2001).
16. F. Pelliccione, A. Micillo, G. Cordeschi, A. D'Angeli, S. Necozione, L. Gandini, A. Lenzi, F. Francavilla, and S. Francavilla, "Altered ultrastructure of mitochondrial membranes is strongly associated with unexplained asthenozoospermia," Fertil. Steril. **95**(2), 641–646 (2011).

Biomedical Optics EXPRESS

17. W. V. Holt, F. Shenfield, T. Leonard, T. D. Hartman, R. D. North, and H. D. Moore, "The value of sperm swimming speed measurements in assessing the fertility of human frozen semen," Hum. Reprod. **4**(3), 292–297 (1989).
18. J. Schindelin, I. Arganda-Carreras, E. Frise, V. Kaynig, M. Longair, T. Pietzsch, S. Preibisch, C. Rueden, S. Saalfeld, B. Schmid, J.-Y. Tinevez, D. J. White, V. Hartenstein, K. Eliceiri, P. Tomancak, and A. Cardona, "Fiji: an open-source platform for biological-image analysis," Nat. Methods **9**(7), 676–682 (2012).
19. G. Joyce, B. D. Robertson, and K. J. Williams, "A modified agar pad method for mycobacterial live-cell imaging," BMC Res. Notes **4**(1), 73 (2011).